ARCHIVES OF ELECTRICAL ENGINEERING VOL. 67(2), pp. 293–306 (2018)

DOI 10.24425/119641

Enhanced IMC synthesis for tracking control of magnetic levitation system

VINODH KUMAR ELUMALAI[1], RAAJA GANAPATHY SUBRAMANIAN[2], JOSHUA SUNDER DAVID REDDIPOGU[1], SOUNDARYA SRINIVASAN[1], SHANTANU AGRAWAL[1]

[1] *VIT University, Vellore, India-632102*

[2] *Eindhoven University of Technology, Eindhoven 5600 MB, The Netherlands*
e-mail: vinothmepsg@gmail.com

(Received: 25.05.2017, revised: 19.02.2018)

Abstract: This paper presents an enhanced internal model control (EIMC) scheme for a time-delayed second order unstable process, which is subjected to exogenous disturbance and model variations. Even though the conventional internal model control (IMC) can provide an asymptotic tracking response with desired stability margins, the major limitation of conventional IMC is that it cannot be applied for an unstable system because a small exogenous disturbance can trigger the control signal to grow unbounded. Hence, modifying the conventional IMC structure to guarantee the internal stability, we present an EIMC scheme which can offer better trade-off between setpoint tracking and disturbance rejection characteristics. To improve the load disturbance rejection characteristics and attenuate the effect of sensor noise, we solve the selection of controller gains as an H_∞ optimization problem. One of the key aspects of the EIMC scheme is that the robustness of the closed loop system can be tuned via a single tuning parameter. The performance of the EIMC scheme is experimentally assessed on a magnetic levitation plant for reference tracking application. Experimental results substantiate that the EIMC scheme can effectively counteract the inherent time delay in the model and offer precise tracking, even in the presence of exogenous disturbance. Moreover, by comparing the trajectory tracking performance of EIMC with that of the proportional integral velocity (PIV) controller through cumulative power spectral density (CPSD) of the tracking error, we show that the EIMC can offer better low frequency servo response with minimal vibrations.

Key words: IMC, magnetic levitation, time delay, Q-parameterization, robustness

1. Introduction

Internal model control (IMC), introduced by Garcia and Morari in 1982, has gained wide acceptance across the process and chemical industries for its simple structure, good tracking feature, and effective tuning philosophy [1]. Relying on the "internal model principle", IMC incorporates the actual and estimated plant model in the design and offers an asymptotically stable

and robust system [2]. IMC offers several key benefits over classical feedback structure. For instance, in the presence of actuator constraints, the performance of classical feedback structure degrades due to the so called integrator windup, whereas IMC does not require any special Anti-windup measures to avoid the saturation problem [3]. Moreover, IMC technique enables the designer to directly specify the desired closed loop time domain performance measures in terms of sensitivity and complementary sensitivity [4].

Several results on the application of IMC in process industries have been reported in the literature. For example, Qiu *et al*. [5], combining the control-relevant identification (plant and its inverse dynamics) with the IMC structure, put forward a composite adaptive IMC (CAIMC) framework to deal with the unmodelled time-varying parameters and validated the performance on a gasoline engine for pressure control application. Li *et al*. [6] assessed the robustness of IMC based PID tuning technique on an atmospheric and vacuum distillation unit, utilizing a stochastic optimization algorithm for controller synthesis. Rivals and Personnaz [7] presented a neural network based internal model control to counteract the time delay effect in stable processes. They exploited the benefits of the neural network particularly, the nonlinear black-box modelling and inverse modelling to cope with model variation. Similarly numerous modified variants of IMC, namely adaptive IMC [8], robust IMC [9] and nonlinear IMC [10] have also been investigated.

However, one of the major limitations with the conventional IMC is that it cannot be applied for a time delayed unstable process because under perfect plant matching condition the IMC acts as an open loop system and a small external perturbation can make the control signal to grow unbounded [11]. Hence, for unstable processes, the conventional IMC structure needs to be modified such that the plant can be stabilized using classical feedback before the standard IMC is applied. Taking cue from this key concept, Tan *et al*. [12] put forward a two-step modified IMC for an unstable plant with time delay. They designed a modified IMC with the assumptions that the plant model is perfect and the sensor noise is absent. However, for real-time control implementation, the modelling error and sensor noise are inevitable. Hence, in this paper, we present an enhanced IMC which can handle the sensor noise and model variation via an additional compensator and assess the performance of enhanced internal model control (EIMC) on a magnetic levitation system. The contributions of this paper are twofold.

1. To cope with the model uncertainty and time delay present in the system, we present a three-stage EIMC design procedure by decoupling the setpoint tracking and disturbance rejection characteristics. To improve the load disturbance characteristics, we solve the selection of controller gains as an optimization problem and augment derivate filters to counteract the effect of sensor noise.
2. The tracking and regulatory performances of the proposed EIMC has been experimentally validated on a benchmark magnetic levitation system. The key feature of the EIMC is that the trade-off between the servo tracking and robustness can be obtained by adjusting a single tuning parameter.

To validate the efficacy of the proposed scheme, three test cases namely combination of multisine servo tracking, regulatory response, and reference following with additional time delay are assessed. Moreover, the tracking performance of the EIMC is compared with that of the PIV controller and the CPSD error of the controller schemes are presented.

The remainder of the paper is organized as follows. Section 2 gives the problem formulation. Section 3 details the conventional IMC design, and section 4 describes the enhanced IMC

structure to deal with the exogenous disturbance and sensor noise. Section 5 presents the mathematical modelling of magnetic levitation plant using the first principles. Section 6 explains the real-time experimental results of EIMC on the magnetic levitation system for trajectory tracking application. Section 7 gives the concluding remarks of the paper.

2. Problem formulation

Consider a second order unstable process with time delay.

$$G(s) = \frac{K}{(\tau_1 s - 1)(\tau_2 s + 1)} e^{-\theta s}, \tag{1}$$

where: K is the steady state gain, τ_1 and τ_2 are the time constants and θ is the time delay. The objective is to design a feedback control scheme based on the extended IMC technique such that the closed loop system is not only robust against exogenous disturbances and model uncertainty but asymptotically stable as given in (2).

$$\lim_{t\to\infty} \|r(t) - y(t)\| = 0, \tag{2}$$

where: $r(t)$ is the reference and $y(t)$ is the response. The challenge of the design is to minimize the tuning parameters involved in the closed loop IMC framework so as to obtain a nominal balance between steady state and transient performance characteristics. Moreover, we aim to extend the enhanced IMC to the tracking control applications of a magnetic levitation system, which is a highly sensitive and unstable process.

3. Conventional IMC

Fig. 1 shows the conventional IMC structure, where G is the process to be controlled $\widetilde{G}$ is the estimated model, Q is the IMC controller, d is the disturbance, r and y are the reference and process output respectively.

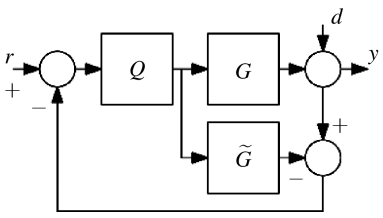

Fig. 1. Conventional IMC scheme

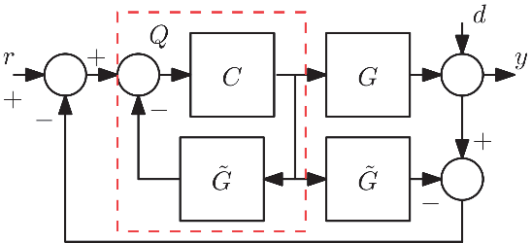

Fig. 2. IMC equivalent classical feedback scheme

The process output is:

$$y = \frac{GC}{1+GC} r + \frac{GC}{1+GC} d. \tag{3}$$

From Fig. 2, which shows the IMC equivalent classical feedback structure, the Q-controller can be represented as:

$$Q = \frac{C}{1+\widetilde{G}C}. \tag{4}$$

Hence, the classical feedback controller is:

$$C = \frac{Q}{1-\widetilde{G}C}. \tag{5}$$

The process output affected by the setpoint tracking and disturbance is given by:

$$y = \frac{GQ}{1+Q(G-\widetilde{G})}r + \frac{1-\widetilde{G}Q}{1+Q(G-\widetilde{G})}d, \tag{6}$$

$$y = Tr + Sd, \tag{7}$$

where: $T = \dfrac{GQ}{1+Q(G-\widetilde{G})}$ is the complementary sensitivity, and $S = \dfrac{\widetilde{G}Q}{1+Q(G-\widetilde{G})}$ is the sensitivity. In the absence of disturbance, if $G = \widetilde{G}$, it is possible to implement perfect control because the complementary sensitivity is reduced to GQ.

$$\frac{y}{r} = GQ. \tag{8}$$

The IMC structure is internally stable if and only if both Q and G are stable. Moreover, for physical realization the Q controller must be causal and proper. According to the well-known two step IMC design procedure, first the process model $\widetilde{G}$ is parameterized into two components such as $\widetilde{G}_+\widetilde{G}_-$ where $\widetilde{G}_+$ represents all non-minimal phase components (RHP zeros and time delay) of the estimated process and $\widetilde{G}_-$ represents all minimal and invertible components. The invertible portion of the model is taken as $\widetilde{Q} = \widetilde{G}_-^{-1}$ to make it stable and causal. Second, an IMC filter is augmented with $\widetilde{Q}$ to ensure the properness of the Q controller.

$$Q = \widetilde{Q}f(s), \tag{9}$$

where $f(s) = \dfrac{1}{(\lambda s+1)^n}$. λ is the tuning parameter, and n is the filter order chosen sufficiently large to guarantee that the number of poles of Q is greater than the no of zeros of Q so as to make the IMC controller proper. The choice of the tuning parameter λ helps in achieving the trade-off between speed of response and robustness of the process. Increasing the value of λ increases the closed loop time constant of the system and increases the robustness of the system against external disturbance. Similarly, decreasing the value of λ improves the speed of response of the system at the cost of reduced robustness against disturbance. Hence, λ can be tuned on-line according to the model mismatch to achieve optimality between the response time and disturbance rejection.

However, the fundamental limitation with the conventional IMC is that it cannot be applied for an unstable process. The standard IMC can be extended for an unstable process if only the control design satisfies the following conditions to guarantee internal stability of the closed loop system.

1. The IMC controller (Q) must be stable, proper and causal.
2. The unstable poles of plant (G) should be nullified by the zeros of Q.

Ensuring these factors during the design phase, we present the enhanced version of IMC, which can overcome the inherent limitations of conventional IMC, through H_∞ optimization based controller synthesis in the following section.

4. Enhanced IMC

The EIMC structure contains four controllers, namely K_0, K_1, K_2 and K_3, with each one has a role and direct effect on the closed loop response as given below.

- K_0 stabilizes the actual unstable plant model G^*, neglecting the time delay.
- K_1 acts as the IMC controller for the stabilized plant model.
- K_2 ensures the internal stability of the EIMC structure by stabilizing the actual unstable plant model with time delay.
- K_3 counteracts the sensor noise and model variation so as to enhance the robustness of the closed loop system.

From the EIMC structure shown in Fig. 3, the process output is:

$$y = \frac{GK_1(1+K_2G^*e^{-\theta s})}{(1+G^*K_0)(1+GK_2)+K_1(G-G^*e^{-\theta s})+GK_3(1+G^*K_0-K_1G^*e^{-\theta s})}r + \\ + \frac{G(1+G^*K_0-K_1G^*e^{-\theta s})}{(1+G^*K_0)(1+GK_2)+K_1(G-G^*e^{-\theta s})+GK_3(1+G^*K_0-K_1G^*e^{-\theta s})}d. \tag{10}$$

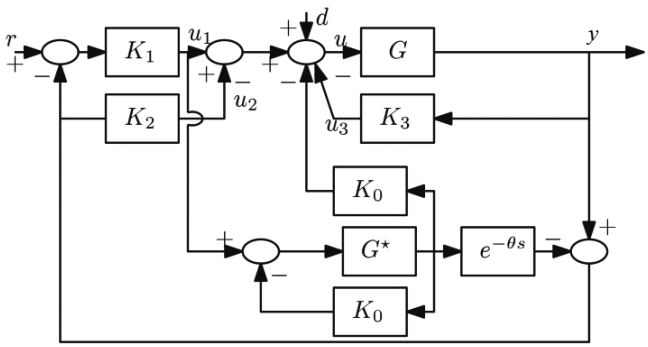

Fig. 3. Enhanced IMC structure

The additional controller gain K_3 will come in to act only during model mismatch and noisy sensor data. In the absence of sensor noise, and exact plant model $G = G^*e^{-\theta s}$, the process output is:

$$y = \frac{GK_1}{1+G^*K_0}r + \frac{G}{1+G^*K_0}\frac{1+G^*K_0-GK_1}{1+G^*K_2}d. \tag{11}$$

Let

$$P^* = \frac{G^*}{1+G^*K_0}, \tag{12}$$

$$P = \frac{G^*}{1+G^*K_0} = G^* e^{-\theta s}. \tag{13}$$

Equation (11) can be rearranged as:

$$y = PK_1 r + \frac{(1-PK_1)G}{1+GK_2} d. \tag{14}$$

Equation (14) indicates that setpoint tracking is independent of K_2. Hence, K_1 acts as the IMC controller if $K_2 = 0$. The key advantage of the EIMC structure is that the setpoint tracking and disturbance rejection are decoupled via independent compensators. Hence, from a practical stand point, tuning the controller gain for improving the tracking performance has less influence over the robustness of the system against disturbance.

The sensitivity transfer function between the disturbance (d) and output (y) is:

$$S_{yd} = \frac{(1-PK_1)G}{1+GK_2}. \tag{15}$$

Similarly, the transfers between the control input (u_2) and the external disturbance (d) is:

$$R_{u_2 d} = \frac{GK_2}{1+GK_2}. \tag{16}$$

The external disturbance d can be rejected by solving the following H_∞ optimization problem.

$$\inf_{K_2} \left\| \frac{W_1 S_{ys}}{W_2 R_{u_2 s}} \right\|_\infty, \tag{17}$$

where W_1 and W_2 are the weights for the input and control sensitivities K_2 respectively. Since representing the control objective in terms of bound on the sensitivity function is practically appealing, the weights corresponding to input and control sensitivities (S_{yd} and $R_{u_2 d}$) are chosen in such a way that they bound the sensitivity function over all frequencies and ensure that the disturbances are not excessively amplified over a magnitude of 6 dB. The following section details the design procedure for tuning the four compensators of EIMC.

4.1. Controller synthesis

Tuning of K_0

From Fig. 3, consider the estimated process model excluding the time delay.

$$\boldsymbol{G}^* = \frac{\boldsymbol{K}}{(\tau_1 \boldsymbol{s}-1)(\tau_2 \boldsymbol{s}+1)}. \tag{18}$$

Since the process has one unstable pole, and one stable pole, selecting K_0 as a PD controller cancels out the unstable pole and yields:

$$P^*(s) = \frac{K}{(\tau_1 s - 1 + KK_0)(\tau_2 s + 1)}. \tag{19}$$

P^* is stable if $K_0 > 1/K$. Hence, selecting $K_0 > 2/K$ makes the estimated model stable as given below.

$$P^*(s) = \frac{K}{(\tau_1 s - 1)(\tau_2 s + 1)}. \tag{20}$$

Tuning of K_1

The stabilized model with time delay is:

$$P^*(s)\, e^{-\theta s} = \frac{K}{(\tau_1 s + 1)(\tau_2 s + 1)} e^{-\theta s}. \tag{21}$$

Augmenting a first order filter with K_1, as given below, ensures that IMC controller is proper.

$$K_1 = \frac{(\tau_1 s + 1)}{K(\lambda s + 1)}. \tag{22}$$

Tuning of K_2

To increase the robustness margins, the controller K_2 is chosen as a PD controller with robust proportional gain K_c and time constant τ_c.

$$K_2 = K_c(\tau_c s + 1), \tag{23}$$

where

$$K_c = \begin{cases} \dfrac{1}{K}\left[\dfrac{0.53}{\theta/\tau_1} + 0.75\right] & \text{if } \theta/\tau_1 \leq 0.7 \\ \dfrac{1}{K}\left[\dfrac{0.51}{\theta/\tau_1} + 0.683\right] & \text{if } 0.7 \leq \theta/\tau_1 \leq 1.5 \end{cases}, \tag{24}$$

$$\tau_c = (0.426\theta/\tau_1 - 0.014)\,\tau_1 + \tau_2. \tag{25}$$

The tuning expressions (24) and (25), which are synthesized based on the time constant of the plant and its time delay, guarantee that the plant dynamics are integrated into the controller computation.

Tuning of K_3

To attenuate the sensor noise, the controller K_3 is modelled as a proportional controller and augmented with second order high pass filter.

$$K_3 = K_p\left(\frac{\omega^2 s}{s^2 + 2\delta\omega s + \omega^2}\right), \tag{26}$$

where δ is the damping ratio and ω is the natural frequency of derivative filter.

5. Magnetic Levitation System

Magnetic levitation technology has received wide attention recently due to its practical importance in many of the engineering applications including high-speed maglev trains, frictionless bearings, vibration isolation in sensitive machine manufacturing, and contactless control in semiconductor manufacturing [13]. Minimizing the physical contact between the stationary and

moving stages, the maglev technology eliminates the friction problem and offers better point to point control for moving masses. The key aspects which enable the industries to utilize the magnetic levitation technology are elimination of the friction problem and better point to point tracking, using contactless control [14].

In this work, we utilize the Quanser's magnetic levitation (maglev) plant to assess the performance of the EIMC framework. A maglev plant contains an electromagnet, a free-floating mass, and a position sensor. Fig. 4 shows the schematic of magnetic levitation plant and Table 1 gives the plant parameters. The entire system is placed in a rectangular enclosure that consists of three distinct sections. The upper section comprises an electromagnet, made of a solenoid coil with a steel core. The middle section contains a chamber where the suspension of the free-floating mass takes place. One of the electromagnet poles faces the top of a black post upon which a one inch steel ball rests. A photo sensor embedded in the post measures the position of free-floating mass. The bottom section of the maglev plant houses the signal conditioning circuit which is needed for conditioning the coil current.

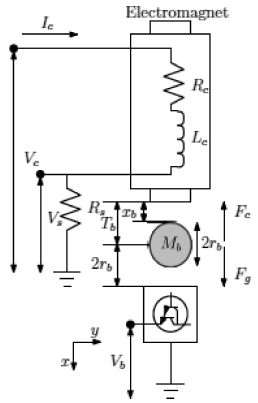

Fig. 4. Schematic of the Maglev plant

Table 1. Magnetic levitation plant parameters

Symbol	Description	Value
R_c	Coil resistance	10 Ω
L_c	Coil inductance	412.5 mH
r_c	Coil steel core radius	8 mm
R_s	Current sense resistance	1 Ω
R_b	Radius of the free-floating mass	0.127 mm
M_b	Free-floating mass	0.068 kg
T_b	Ball travel	9 mm
g	Gravitational constant	9.81 m/s^2
K_b	Ball position sensor sensitivity	2.83 mm/V
K_m	Electromagnet force constant	0.653 μN.m^2/A^2

5.1. Mathematical Modelling

The attractive force F_c acting on the mass due to the electromagnet is:

$$F_c = \frac{K_m I_c(t)^2}{2x_b(t)^2}, \tag{27}$$

where: x_b is the position of floating mass and K_m is the electromagnetic force constant. Similarly, the opposing force F_g acting on the mass due to gravity is:

$$F_g = M_b g. \tag{28}$$

Hence, according to Newton's second law, the total force experienced by the free-floating mass is:

$$F_{\text{ext}} = -F_c + F_g \Rightarrow M_b x_b(t) = \frac{K_m I_c(t)^2}{2x_b(t)^2} + M_b g. \tag{29}$$

Therefore, the nonlinear equation of motion (EoM) of the floating mass is:

$$\ddot{x}_b(t) = -\frac{K_m I_c(t)^2}{2M_b x_b(t)^2} + g. \tag{30}$$

We can obtain the following transfer function of the magnetic levitation system about the equilibrium point (x_{b0}, I_{c0}) by linearizing (30) using the Taylor's series.

$$G_b(s) = \frac{\Delta x_b(s)}{\Delta I_b(s)} = \frac{K_b \omega_n^2}{s^2 - \omega_b^2} \tag{31}$$

where: $K_b = \dfrac{x_{b0}}{I_{c0}}$ is the steady-state gain, and $\omega_b = \sqrt{\dfrac{2g}{x_{b0}}}$ is the natural frequency. The transfer function (31) highlights that the open loop subsystem formed by free-floating mass is unstable due to the presence of a pole in the right half of imaginary axis. Hence, the maglev plant needs a feedback controller to stabilize the plant.

6. Experimental Results and Discussion

The experimental test-bed, as shown in Fig. 5, consists of a personal computer, maglev plant, two channel data acquisition board (DAQ) and a signal conditioning circuit. The DAQ board, which has an input range of ± 10 V and a resolution of 12 bit, can measure signals until 0.5 kHz control rate. A power amplifier which can provide a regulated supply of ± 10 V at 3 A governs the current supplied to the electromagnet. For hardware in loop (HIL) testing, the control algorithm implemented in Simulink interacts with the Quanser real-time control (QUARC) software. The control objective is to make the mass float freely and follow the reference trajectory by controlling the current supplied to the electromagnet.

We can obtain the following time delayed ($\theta = 1$ ms) transfer function model of the magnetic levitation system by substituting the plant parameters given in Table 1 into (31).

$$G(s) = -\frac{0.007}{(0.0175s - 1)(0.0175s + 1)}. \tag{32}$$

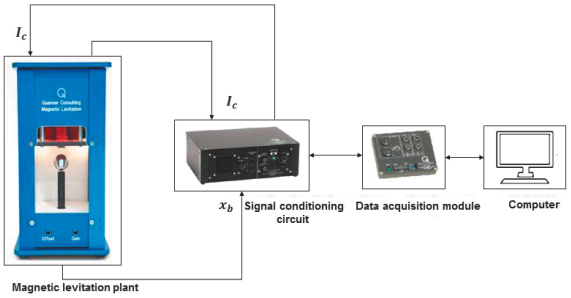

Fig. 5. Experimental testbed

The time constants and the steady state gain of the plant are $0.0175s$ and $0.007s$ respectively. The four compensator gains of the EIMC structure, tuned as given in section 4, are as follows:

$$K_0 = -285.92(0.175s+1), \tag{33}$$

$$K_1 = -\frac{(0.0175s+1)}{0.007(0.2s+1)}, \tag{34}$$

$$K_2 = -239.92(0.0215s+1), \tag{35}$$

$$K_3 = -1.3\left[\frac{222066s}{s^2+848.23s+222066}\right]. \tag{36}$$

The efficacy of the EIMC is validated through three test cases namely, servo tracking, regulatory response, and tracking with additional time delay.

6.1. Servo tracking

In real time scenario, the maglev system should adapt not only to directional changes but to variations in the magnitude as well. Hence, we utilized the following multi-sine test pattern to validate the reference following capability of EIMC.

$$r = \begin{cases} 14, & t = 0, \\ T_b + \sin(2\pi 0.015t) + 0.5\sin(2\pi 0.5t + \sin 2\pi 0.7t), & t > 0, \end{cases} \tag{37}$$
$$\text{s.t.,}\ |\dot{r}| \leq 5\ \text{mm}.$$

To avoid sudden jump, the floating mass initially begins at T_b and gradually follows the combination of sine patterns. Fig. 6, which shows the tracking response along with the respective control input and tracking error, highlights that the EIMC can make the free-floating mass track even the multi-sine reference pattern, which is highly challenging due to its sudden varying nature and combination of three different frequencies. The maximum tracking error of 0.014 mm during the initial transient phase and 0.004 mm peak to peak during tracking substantiates that EIMC can offer good reference following response even with the challenging reference signal. The control input, coil current (I_c), plot shows that the precise control is implemented for the position control of free-floating mass.

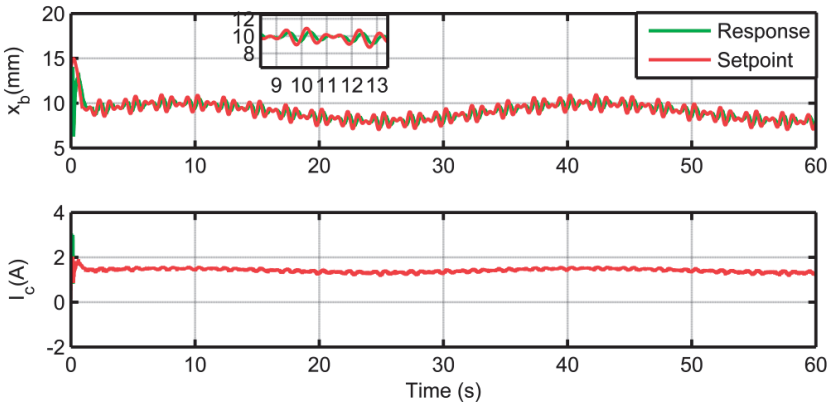

Fig. 6. Servo tracking response for multi-sine test signal

6.2. Steady state performance evaluation

A constant setpoint of 9 mm is given as a test signal and an external impulse disturbance with a magnitude of 0.2 mm is introduced into the system from $t = 20$ s to $t = 22$ s. The effect of tuning parameter (λ) on tracking and rejecting the external disturbance is assessed for two test cases, namely 0.17 and 0.2. From Fig. 7, which shows the regulatory response, we can read that with $\lambda = 0.2$ the EIMC offers increased robustness against the external disturbance compared to the tracking response of $\lambda = 0.17$. The response indeed proves that increasing the value of tuning parameter improves the disturbance rejection (robustness) property by reducing the deviation from steady state to a minimum level, whereas the smaller values of tuning parameter focuses on reference tracking by bringing the trajectory quickly to steady state even in the presence of disturbance.

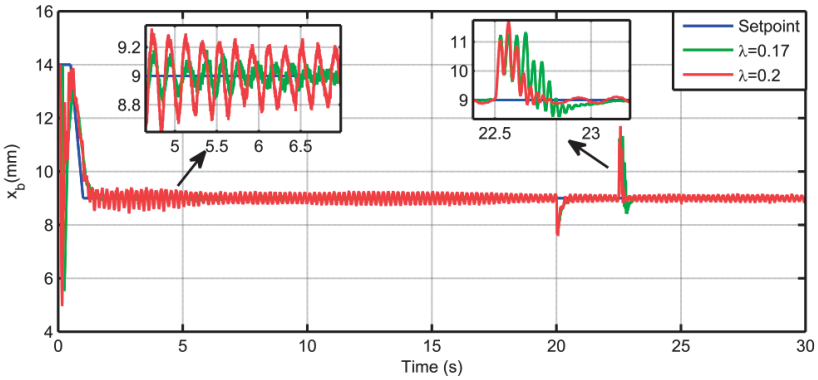

Fig. 7. Regulatory response

6.3. Tracking with additional time delay

One of the key features of the EIMC methodology is that the inherent time delay present in the maglev system is also considered in the controller design to combat the effect of delayed control

signal. Two test cases with additional time delays $\theta = 10$ ms and $\theta = 30$ ms are considered for analysis. Fig. 8 shows the tracking performance of the EIMC along with their control signal and tracking error. Since the critical gain K_2 is chosen based on the time delay and time constant of the system, the oscillations in the position of free-floating mass even with higher time delay of $\theta = 30$ ms is maintained within the nominal range of 1 mm by compensating the delayed response through controlled coil current.

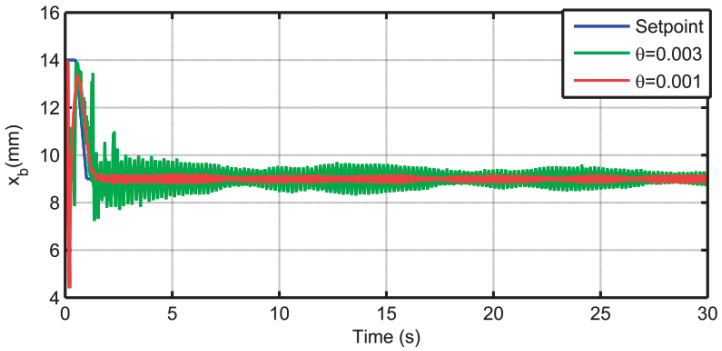

Fig. 8. Tracking with time delay

6.4. Discussion: Performance validation

Finally, for validation, the tracking efficiency of EIMC is compared with that of the PIV controller put forward in [15]. Fig. 9, which shows the reference tracking responses of both EIMC and PIV, proves that even though during the initial transient phase the tracking response of EIMC drops faster from the desired setpoint compared to that of PIV, EIMC offers a good steady state tracking response with lesser deviation in state trajectory compared to PIV. Moreover, to assess the tracking features, the CPSD of tracking error for the two controllers are illustrated in Fig. 10. The CPSD of the error is calculated as a summation of FFT of the tracking error and its root mean square. It is worth to note that even though CPSD of EIMC is slightly larger in

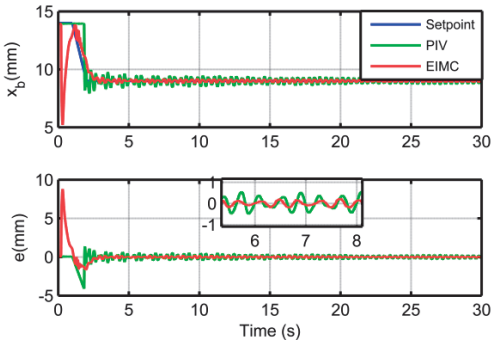

Fig. 9. Servo tracking of EIMC and PIV

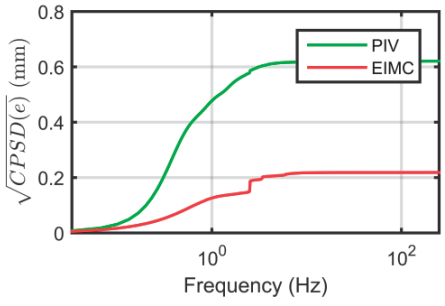

Fig. 10. CPSD of error for PIV and EIMC

the high-frequency region due to the sudden drop of the position of the floating mass from its setpoint compared to that of PIV, the low-frequency performance of EIMC is better than that of PIV.

7. Conclusions

This paper has presented an EIMC structure which can offer improved robustness against exogenous disturbance and model variation for a second order unstable process with time delay. Modifying the Q-parameterization of conventional IMC structure as a combination of four compensators, we have presented an EIMC framework, which can offer better trade-off between servo and regulatory performance through a single tuning parameter. The selection of controller gains to reject the load disturbance has been solved using H_∞ optimization problem and the derivative filters have been augmented with the controller to attenuate the performance deterioration due to sensor noise. The performance of the EIMC scheme has been validated on a magnetic levitation plant for reference following application. Three test cases namely setpoint tracking under the presence of multi-sine reference signal, regulatory response, and tracking under explicitly time delayed control signal have been assessed. The experimental results accentuate that the EIMC can offer better servo and regulatory performance compared to a conventional PIV scheme.

References

[1] Yadav A.K., Gaur P., *Intelligent modified internal model control for speed control of nonlinear uncertain heavy duty vehicles*, ISA Transactions, vol. 56, pp. 288–298 (2015).

[2] Zhu H.A, Hong G.S., Teo C.L., Poo A.N., *Internal model control with enhanced robustness*, International Journal of Systems Science, vol. 26, no. 2, pp. 277–293 (1995).

[3] Jin Q.B., Liu Q., *Analytical IMC-PID design in terms of performance/robustness trade-off for integrating processes: From 2-Dof to 1-Dof*, Journal of Process Control, vol. 24, no. 3, pp. 22–32 (2014).

[4] Wang Q., Lu C., Pan W., *IMC PID controller tuning for stable and unstable processes with time delay*, Chemical Engineering Research and Design, vol. 105, pp. 120–129 (2016).

[5] Qiu Z., Santillo M., Jankovic M., Sun J., *Composite Adaptive Internal Model Control and Its Application to Boost Pressure Control of a Turbocharged Gasoline Engine*, IEEE Transactions on Control Systems Technology, vol. 23, no. 6, pp. 2306–2315 (2015).

[6] Li D., Zeng F., Jin Q., Pan L., *Applications of an IMC based PID Controller tuning strategy in atmospheric and vacuum distillation units*, Nonlinear Analysis: Real World Applications, vol. 10, pp. 2729–2739 (2009).

[7] Rivals I., Personnaz L., *Nonlinear Internal Model Control Using Neural Networks: Application to Processes with Delay and Design Issues*, IEEE Transactions on Neural Networks, vol. 11, no. 1, pp. 80–90 (2000).

[8] Rupp D., Guzzella L., *Adaptive internal model control with application to fueling control*, Control Engineering Practice, vol. 18, no. 8, pp. 873–881 (2010).

[9] Clergeta C.H., Grimaldia J.P., Chebre M., Petit N., *An example of robust internal model control under variable and uncertain delay*, Journal of Process Control, vol. 60, pp. 4–23 (2017).

[10] Bouzid Y., Siguerdidjane H., Bestaoui H., *Nonlinear internal model control applied to VTOL multirotors UAV*, Mechatronics, vol. 47, pp. 49–66 (2017)

[11] Morari M., Zarifiriou E., *Robust process control*, Prentice hall, New Jersey (1989).

[12] Tan W., Marquez H.J., Chen T., *IMC design for unstable processes with time delays*, Journal of Process Control, vol. 13, no. 3, pp. 203–213 (2003).

[13] Elumalai V.K., Jerome J., *Algebraic Riccati equation based Q and R matrices selection algorithm for optimal LQR applied to tracking control of 3rd order magnetic levitation system*, Archives of Electrical Engineering, vol. 65, no. 1, pp. 151–168 (2016).

[14] Butler H., *Position control in lithographic equipment: an enabler for current-day chip manufacturing*, IEEE Transactions on Control Systems, vol. 31, no. 5, pp. 28–47 (2011).

[15] Elumalai V.K., Jerome J., *LQR based Optimal Tuning of PID Controller for Trajectory Tracking of Magnetic Levitation System*, Procedia Engineering, vol. 64, pp. 654–664, 2013.